Effective conductivities of two-phase composites with a singular phase

Liping Liu[a)]
Department of Mechanical Engineering, University of Houston, Houston, Texas 77204, USA

(Received 17 January 2009; accepted 3 March 2009; published online 18 May 2009)

We calculate the effective conductivity of a two-phase composite with a periodic array of inhomogeneities. The shape of the inhomogeneities is assumed to be a periodic E-inclusion. The effective conductivity is expressed in terms of the volume fraction of the inhomogeneities and a matrix, which characterizes the shape of the periodic E-inclusion. This solution is rigorous, closed-form, and applicable to situations that the conductivity of the inhomogeneities is singular, i.e., zero or infinite. Further, when the periodic E-inclusion degenerates to a periodic array of slits with vanishing volume fraction, we give explicit solutions to local fields and effective conductivity of the composite with singular inhomogeneities. © *2009 American Institute of Physics*. [DOI: 10.1063/1.3110026]

I. INTRODUCTION

High-contrast composites have wide industrial applications. Examples include metal and glass foams, fibrous metal and glass materials, fiber-reinforced materials, and fractured porous media. Once the notion of effective properties of composites or heterogeneous media is established, we are faced with the critical problem of finding the effective properties of a given composite and, if possible, relating the effective properties with the microstructure of the composite. However this is difficult even for composites with simple microstructures, for example, a two-phase composite with a periodic array of inhomogeneous spheres. In this and similar cases, heuristic methods such as the effective medium theory (Ref. 1 and references therein) and the self-consistent method[2] can give us closed-form formulas of the effective properties. These approximate formulas are in good agreement with experiments when the contrast between the two phases is small but unsatisfactory when the contrast of the constituent phases becomes large. If we idealize the physical properties of the inhomogeneities to be infinite or zero, many of the approximate formulas even yield unphysical results. Further, rigorous bounds such as the Hashin–Shtrikman bounds[3] are not of much use since they are far apart from each other for high-contrast composites. So it is important for both theory and application to have a reasonable estimate of the effective properties of high-contrast composites. This is the purpose of this paper.

Theoretical results are available for a small number of particular cases in the literature. Keller[4] considered a composite of a cubic array of perfectly conducting spheres embedded in a normal conducting medium and obtained an asymptotic formula for the effective conductivity when the gaps between nearby spheres are small. Dykne[5] showed that a two-phase system of insulating and conducting materials could undergo a dielectrics-conductor transition at certain critical concentration. For random high-contrast composites, a number of authors[6,7] used a discrete network to model a high-contrast composite based on physical consideration. Kozlov[8] and Berlyand and Kolpakov[9] showed that the discrete network is a sound model of the original continuum problem. From these works, we observe that high-contrast composites have two distinguishing features compared with normal composites. The first is that high-contrast composites can undergo a percolation transition, and the second is that the effective properties are dependent on the local geometry of the composite, say, the interinhomogeneity distance, as much as the global parameter, such as the volume fraction. In particular, if the physical property of the inhomogeneities is zero or infinite, the inhomogeneities could have a significant impact on the effective properties even if their volume fraction vanishes. This is well understood in the context of fracture mechanics[10,11] but seems unnoticed for conductive composites.

In this paper we give explicit solutions to the effective properties of a class of periodic composites. To obtain these solutions we choose a special class of microstructures called periodic E-inclusions or Vigdergauz[12] structures in two dimensions.[13] Unlike previous examples, our solutions are rigorous and closed-form, which express the effective properties in terms of the volume fraction θ of the inhomogeneities and the matrix $\mathbf{Q}$, which characterizes the shape of the inhomogeneities. A disadvantage of our solutions is that the shape of periodic E-inclusions is not directly given; we need to solve a variational inequality to find a periodic E-inclusion.[13,14] Nevertheless, without solving the variational inequality we know qualitatively the shapes of periodic E-inclusions and how they depend on the volume fraction θ and the shape matrix $\mathbf{Q}$. In particular, when the shape matrix $\mathbf{Q}$ is singular and the volume fraction θ approaches to zero, the periodic E-inclusion degenerates to a slit in two dimensions. In this case we express the effective properties in terms of the length of the slit. It indicates that the widely used rules of mixtures, which interpolate between the properties of the matrix and the inhomogeneities by volume fractions, could be qualitatively misleading for high-contrast composites.

Two remarks are in order here about the scope of this paper. For simplicity we discuss the conductivity problem,

[a)]Electronic mail: liuliping@uh.edu.

but note that the solutions are applicable to other physical properties including dielectric properties, diffusive properties, transport properties, and at least qualitatively, elastic properties. More, our solutions are for periodic composites. Therefore, the effects of percolation and randomness are not addressed here.

The paper is organized as follows. In Sec. II we formulate the governing equation for a periodic composite and derive the formulas for calculating the effective properties of the composite. In Sec. III we define the periodic *E*-inclusion and show how to calculate the effective properties of a composite with a periodic *E*-inclusion microstructure. In Sec. IV we discuss a particular situation that the periodic *E*-inclusion degenerates to a periodic array of slits. For this particular situation we give explicit solutions to local fields and effective properties for a rectangular lattice in Sec. IV A and for a rhombic lattice in Sec. IV B. Finally we summarize our results in Sec. V.

II. PROBLEM FORMULATION

Let $Y \subset IR^n$ be a unit cell associated with a Bravais lattice $\mathcal{L}$, $\Omega \subset Y$ be an inclusion containing an inhomogeneity, and θ be the volume fraction of the inhomogeneities. Consider a periodic two-phase composite with conductivity given by

$$\mathbf{A}(\mathbf{x}) = \begin{cases} k_0\mathbf{I} & \text{if } \mathbf{x} \in Y\setminus\Omega \\ k_1\mathbf{I} & \text{if } \mathbf{x} \in \Omega, \end{cases} \tag{1}$$

where $k_0 > 0$, $k_1 \geq 0$, and $\mathbf{I} \in IR^{n\times n}$ is the identity matrix. For ease of terminology, we refer to phase-0 as the matrix and phase-1 as the inhomogeneities. From the homogenization theory,[15] the effective conductivity of the composite, described by a symmetric tensor $\mathbf{A}^e$, is given by

$$\mathbf{f}\cdot\mathbf{A}^e\mathbf{f} = \min_{u\in\mathbb{W}} ⨍_Y (\nabla u + \mathbf{f})\cdot\mathbf{A}(\mathbf{x})(\nabla u + \mathbf{f}), \tag{2}$$

where $⨍_V = (1/|V|)\int_V$ denotes the average of the integrand over V ($|V|$ denotes the volume of V), $\mathbf{f} \in IR^n$ is the average applied field, and the admissible space $\mathbb{W}$ is the collection of all periodic square integrable functions $u: IR^n \to IR$ whose gradients remain square integrable. To evaluate the effective conductivity tensor $\mathbf{A}^e$, we need to solve the Euler–Lagrange equation of Eq. (2) for the minimizer $u_{\mathbf{f}}$,

$$\begin{cases} \mathrm{div}[\mathbf{A}(\mathbf{x})(\nabla u_{\mathbf{f}} + \mathbf{f})] = 0 \ \text{ on } \ Y, \\ \text{periodic boundary conditions on } \ \partial Y, \end{cases} \tag{3}$$

and then compute the integral for $u = u_{\mathbf{f}}$ on the right hand side of Eq. (2).

The effective conductivity of a composite can be expressed as a boundary integral of the minimizer $u_{\mathbf{f}}$ or an integral on one of the phases. To see this, we notice $u_{\mathbf{f}}$ being a periodic function and $\mathbf{A}(\mathbf{x})(\nabla u_{\mathbf{f}} + \mathbf{f})$ being divergence-free imply

$$⨍_Y \nabla u_{\mathbf{f}} = 0 \quad \text{and} \quad ⨍_Y \nabla u_{\mathbf{f}}\cdot\mathbf{A}(\mathbf{x})(\nabla u_{\mathbf{f}} + \mathbf{f}) = 0. \tag{4}$$

Therefore, we have

$$\begin{aligned} \mathbf{f}\cdot\mathbf{A}^e\mathbf{f} &= ⨍_Y (\nabla u_{\mathbf{f}} + \mathbf{f})\cdot\mathbf{A}(\mathbf{x})(\nabla u_{\mathbf{f}} + \mathbf{f}) \\ &= ⨍_Y \mathbf{f}\cdot\mathbf{A}(\mathbf{x})(\nabla u_{\mathbf{f}} + \mathbf{f}) = \mathbf{f}\cdot ⨍_Y (\nabla\mathbf{x})\mathbf{A}(\mathbf{x})(\nabla u_{\mathbf{f}} + \mathbf{f}) \\ &= \frac{1}{|Y|}\int_{\partial Y} (\mathbf{f}\cdot\mathbf{x})\mathbf{n}\cdot\mathbf{A}(\mathbf{x})(\nabla u_{\mathbf{f}} + \mathbf{f}), \end{aligned} \tag{5}$$

where $\mathbf{n}$ is the outward normal on ∂Y. Alternatively, from the first line in Eq. (5) we find

$$\begin{aligned} \mathbf{f}\cdot\mathbf{A}^e\mathbf{f} &= k_0 ⨍_Y \mathbf{f}\cdot(\nabla u_{\mathbf{f}} + \mathbf{f}) + (k_1 - k_0)\mathbf{f}\cdot\theta ⨍_\Omega (\nabla u_{\mathbf{f}} + \mathbf{f}) \\ &= k_0|\mathbf{f}|^2 + (k_1 - k_0)\mathbf{f}\cdot\left[\mathbf{f} - (1-\theta) ⨍_{Y\setminus\Omega} (\nabla u_{\mathbf{f}} + \mathbf{f})\right]. \end{aligned} \tag{6}$$

For general inclusions, we do not have a closed-form solution of Eq. (2), and thus much of the works have been focused on the bounds on the effective conductivity tensor $\mathbf{A}^e$ and numerical methods that compute $\mathbf{A}^e$ for a given inclusion Ω. An exception is the case that the inclusion Ω is a periodic *E*-inclusion. Below we describe what a periodic *E*-inclusion is and calculate the effective conductivity of a composite with the inclusion being a periodic *E*-inclusion.

III. EFFECTIVE CONDUCTIVITIES OF COMPOSITES WITH PERIODIC *E*-INCLUSION INHOMOGENEITIES

Recently, the Liu *et al.*[16] found a class of special inclusions for which a closed-form solution of Eq. (2) is available. These special inclusions, termed as *periodic E*-inclusions, are defined as an inclusion $\Omega \subset Y$ such that the overdetermined problem

$$\begin{cases} \Delta\xi = \theta - \chi_\Omega \ \text{ on } \ Y, \\ \nabla\nabla\xi = -(1-\theta)\mathbf{Q} \ \text{ on } \ \Omega, \\ \text{periodic boundary conditions on } \ \partial Y \end{cases} \tag{7}$$

admits a solution where χ_Ω is the characteristic function of Ω and

$$\mathbf{Q} \in \mathbb{Q} := \{\mathbf{M} \in IR^{n\times n}_{\text{sym}}: \mathbf{M} \text{ is positive semidefinite with } \mathrm{Tr}(\mathbf{M}) = 1\}. \tag{8}$$

The Liu *et al.*[13] showed the existence of periodic *E*-inclusions for any volume fraction $\theta \in (0,1)$, any matrix $\mathbf{Q} \in \mathbb{Q}$, and any Bravais lattice $\mathcal{L}$. Figure 1 shows three examples of periodic *E*-inclusions in two dimensions (see Refs. 17, 16, and 13 for more examples). We remark that periodic *E*-inclusions are generalizations of two-dimensional structures constructed by Vigdergauz.[12]

If the inclusion Ω for the composite is a periodic *E*-inclusion with matrix $\mathbf{Q}$ and volume fraction θ, we claim that a solution of Eq. (3) is given by

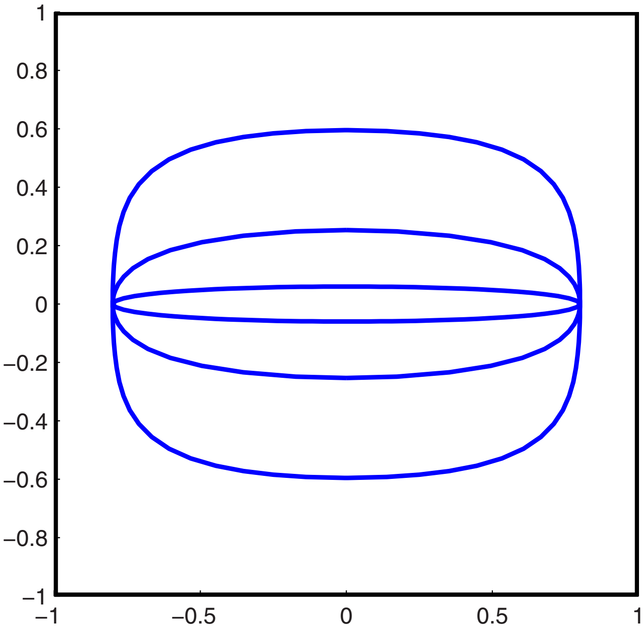

FIG. 1. (Color online) From outward to inward, the regions bounded by the curves are periodic E-inclusions with matrices $\mathbf{Q}$ and volume fractions θ given by Eq. (16) and unit cell $Y=(-1,1)^2$.

$$u_{\mathbf{f}}=\mathbf{a}\cdot\nabla\xi, \quad \mathbf{a}=(k_1-k_0)[(1-\theta)(k_1-k_0)\mathbf{Q}+k_0\mathbf{I}]^{-1}\mathbf{f}. \tag{9}$$

To see this, we notice that for Eq. (3) the interfacial condition on $\partial\Omega$ can be written as

$$k_1\mathbf{n}\cdot[\nabla u_{\mathbf{f}}(\mathbf{x}-)+\mathbf{f}]=k_0\mathbf{n}\cdot[\nabla u_{\mathbf{f}}(\mathbf{x}+)+\mathbf{f}] \quad \forall\ \mathbf{x}\in\partial\Omega, \tag{10}$$

whereas ξ being a solution of $\Delta\xi=\theta-\chi_\Omega$ satisfies

$$\nabla\nabla\xi(\mathbf{x}-)-\nabla\nabla\xi(\mathbf{x}+)=-\mathbf{n}\otimes\mathbf{n} \quad \forall\ \mathbf{x}\in\partial\Omega, \tag{11}$$

where $\mathbf{n}$ is the outward normal on $\partial\Omega$ and $\mathbf{x}-$ $(\mathbf{x}+)$ denotes the limit from the inside (outside) of Ω. From Eq. (11) and the second of Eq. (7), direct calculation reveals that for any $\mathbf{a}\in IR^n$,

$$\begin{aligned}k_0\mathbf{n}\cdot[\nabla\mathbf{a}\cdot\nabla\xi(\mathbf{x}+)+\mathbf{f}] &= k_1\mathbf{n}\cdot[-(1-\theta)\mathbf{Q}\mathbf{a}+\mathbf{f}]-k_1[-(1-\theta)\mathbf{n}\cdot\mathbf{Q}\mathbf{a}+\mathbf{n}\cdot\mathbf{f}]\\ &\quad +k_0[-(1-\theta)\mathbf{n}\cdot\mathbf{Q}\mathbf{a}+\mathbf{a}\cdot\mathbf{n}+\mathbf{n}\cdot\mathbf{f}]\\ &= k_1\mathbf{n}\cdot[\nabla\mathbf{a}\cdot\nabla\xi(\mathbf{x}-)+\mathbf{f}]\\ &\quad +\mathbf{n}\cdot[(k_1-k_0)(1-\theta)\mathbf{Q}\mathbf{a}+k_0\mathbf{a}+(k_0-k_1)\mathbf{f}].\end{aligned} \tag{12}$$

Therefore, if we choose the vector $\mathbf{a}$ as in Eq. (9), the last term on the right hand side of Eq. (12) vanishes, and hence $u_{\mathbf{f}}=\mathbf{a}\cdot\nabla\xi$ satisfies the interfacial condition (10). Further, we can easily verify that $u_{\mathbf{f}}=\mathbf{a}\cdot\nabla\xi$ satisfies the first of Eq. (3) on the interior and exterior of Ω and the periodic boundary conditions on ∂Y. We thus conclude that $u_{\mathbf{f}}=\mathbf{a}\cdot\nabla\xi$ is a solution of Eq. (3) if Ω is a periodic E-inclusion and ξ is given by Eq. (7).

Using Eq. (9) we can calculate the effective conductivity tensor $\mathbf{A}^e$ for a periodic E-inclusion. By the first line of Eq. (6) and the second of Eq. (7) we find

$$\mathbf{A}^e=k_0\mathbf{I}+\theta(k_1-k_0)\mathbf{I}-\theta(1-\theta)(k_1-k_0)^2\mathbf{Q}[(1-\theta)(k_1-k_0)\mathbf{Q}+k_0\mathbf{I}]^{-1}. \tag{13}$$

We remark that the above formula is rigorous and attains the lower (upper) Hashin–Shtrikman[3] bound if $k_0<k_1$ $(k_0>k_1)$. It has a few regimes that need separate attention.

(1) If k_1 is nonsingular, i.e., $\neq 0$ or $+\infty$, formula (13) gives a definite answer to the effective conductivity tensor of the composite of a periodic E-inclusion with any matrix $\mathbf{Q}\in\mathbb{Q}$ and any volume fraction $\theta\in[0,1]$ since $(1-\theta)\times(k_1-k_0)\mathbf{Q}+k_0\mathbf{I}$ is invertible. In particular, if we assume the composite is isotropic, then the corresponding matrix $\mathbf{Q}$ is equal to $\mathbf{I}/n$. Denoting by k^e the isotropic conductivity of the composite, from Eq. (13) we have

$$\frac{k^e}{k_0}=\frac{(1-\theta)(n-1)+[1+\theta(n-1)]k_1/k_0}{n-1+\theta+(1-\theta)k_1/k_0}. \tag{14}$$

(2) If $\mathbf{Q}$ is positive definite, formula (13) also gives a definite answer even if k_1 is singular. In particular, we have

$$\mathbf{A}^e/k_0=(1-\theta)\mathbf{I}-\theta(1-\theta)\mathbf{Q}[-(1-\theta)\mathbf{Q}+\mathbf{I}]^{-1} \ \text{ if } \ k_1=0,$$

$$\mathbf{A}^e/k_0=\mathbf{I}+\frac{\theta}{1-\theta}\mathbf{Q}^{-1} \ \text{ if } \ k_1=+\infty. \tag{15}$$

The second of the above formula follows from the fact that as $k_1\to+\infty$,

$$\left[(1-\theta)\mathbf{Q}+\frac{k_0}{k_1-k_0}\mathbf{I}\right]^{-1} = \frac{1}{1-\theta}\mathbf{Q}^{-1}-\frac{k_0}{(1-\theta)^2(k_1-k_0)}\mathbf{Q}^{-1}\mathbf{Q}^{-1} + O\left(\left|\frac{k_0}{k_1-k_0}\right|^2\right).$$

If the composite is assumed to be isotropic with the effective conductivity denoted by k_0^e (k_∞^e) for $k_1=0$ $(k_1=+\infty)$, then from Eq. (14) or Eq. (15) we have

$$\frac{k_0^e}{k_0}=\frac{(1-\theta)(n-1)}{n-1+\theta}, \quad \frac{k_\infty^e}{k_0}=\frac{1+(n-1)\theta}{1-\theta}.$$

(3) If $\theta\in(0,1]$, $\mathbf{Q}$ is singular, and $k_1=0$ or $+\infty$, formula (15) yields a definite answer to $\mathbf{A}^e$ if we interpret the inverse of a matrix $\mathbf{M}\in IR^{n\times n}$ as

$$\mathbf{M}^{-1}=\lim_{\varepsilon\searrow 0}[\mathbf{M}+\varepsilon\mathbf{I}]^{-1}.$$

(4) If $\theta=0$ and $\mathbf{Q}$ is singular, formula (15) is not necessarily meaningful since we could get a term such as $0\cdot\infty$. Nevertheless, such situations are physically interesting. Below we focus on this regime in two dimensions.

IV. EFFECTIVE CONDUCTIVITIES OF COMPOSITES WITH PERIODIC SLIT INHOMOGENEITIES

In this section we restrict ourselves to two dimensions $(n=2)$. From the viewpoint of last section and in connection with geometry, we are interested in the following limit: we fix the two ends of the periodic E-inclusion Ω along x_1-direction and let the dimension of Ω along x_2-direction shrink to zero. Using formulas in Refs. 17 and 16, we plot three periodic E-inclusions in two dimensions for unit cell $Y=(-1,1)^2$ in Fig. 1. From outward to inward, the matrix $\mathbf{Q}$ and volume fraction θ are given by

$$\mathbf{Q}=\begin{bmatrix}\frac{r}{1+r} & 0\\ 0 & \frac{1}{1+r}\end{bmatrix},\quad r=0.5,\ 0.2,\ 0.01 \quad\text{and}\quad \theta = 0.42,\ 0.17,\ 0.04. \tag{16}$$

We note that as

$$\mathbf{Q}\to\begin{bmatrix}0 & 0\\ 0 & 1\end{bmatrix} \quad\text{and}\quad \theta\to 0,$$

the periodic E-inclusion approaches to a slit parallel to x_1-axis. Our goal is to compute the effective conductivity $\mathbf{A}^e$ in this limit for singular k_1, for which Eq. (13) or Eq. (15) is no longer applicable. If k_1 is a finite positive number, from Eq. (13) we have $\mathbf{A}^e=k_0\mathbf{I}$, as expected.

To proceed, we reformulate problem (3) for $k_1=+\infty$ or 0. If $k_1=+\infty$, the inclusion Ω necessarily remains as an equipotential body, and so problem (3) is equivalent to

$$\begin{cases}\Delta u_{\mathbf{f}}=0 \ \text{ on } \ Y\setminus\bar{\Omega},\\ \mathbf{t}\cdot(\nabla u_{\mathbf{f}}+\mathbf{f})=0 \ \text{ on } \ \partial\Omega,\\ \text{periodic boundary conditions on } \partial Y,\end{cases} \tag{17}$$

where $\mathbf{t}$ is the tangent on $\partial\Omega$. Since Ω is a slit parallel to x_1-axis, the second of Eq. (17) can be rewritten as

$$\frac{\partial u_{\mathbf{f}}(x_1,x_2)}{\partial x_1}+f_1=0 \qquad \forall\,(x_1,x_2)\in\partial\Omega. \tag{18}$$

If $k_1=0$, from the Gaussian theorem we infer that problem (3) is equivalent to

$$\begin{cases}\Delta u_{\mathbf{f}}=0 \ \text{ on } \ Y\setminus\bar{\Omega},\\ \mathbf{n}\cdot(\nabla u_{\mathbf{f}}+\mathbf{f})=0 \ \text{ on } \ \partial\Omega,\\ \text{periodic boundary conditions on } \partial Y.\end{cases} \tag{19}$$

Since Ω is a slit parallel to x_1-axis, the second of Eq. (19) can be rewritten as

$$\frac{\partial u_{\mathbf{f}}(x_1,x_2)}{\partial x_2}+f_2=0 \qquad \forall\,(x_1,x_2)\in\partial\Omega. \tag{20}$$

We will give explicit solutions to Eqs. (17) and (19) for a rectangular or a rhombic unit cell using *Weierstrass elliptic functions*. In complex analysis, we denote by $z=x_1+ix_2$ $(x_1,x_2\in IR)$ a point on the complex plane $\mathbb{C}$. We identify the complex plane $\mathbb{C}$ with IR^2 in this obvious manner. Let $2\omega_1,2\omega_3\in\mathbb{C}$ with $\mathrm{Im}[\omega_1/\omega_3]\neq 0$ be the periods and

$$\mathcal{L}=\{2\nu_1\omega_1+2\nu_2\omega_3 : \nu_1,\nu_2\in\mathbb{Z}\} \tag{21}$$

be the lattice. Associated with this lattice, we denote by Y the open parallelogram with vertices 0, $2\omega_1$, $2\omega_2=2(\omega_1+\omega_3)$, and $2\omega_3$ and recall that the Weierstrass $\wp$-function

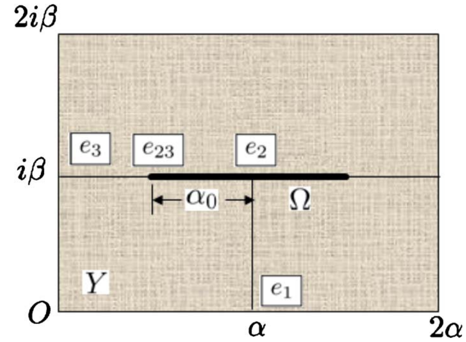

FIG. 2. (Color online) Rectangular unit cell.

$$\wp(z|\omega_1,\omega_3)=\frac{1}{z^2}+\sum_{\omega\in\mathcal{L}\setminus\{0\}}\left[\frac{1}{(z-\omega)^2}-\frac{1}{\omega^2}\right] \tag{22}$$

is Y-periodic, analytic on Y, has a second-order pole at every lattice point in $\mathcal{L}$, and takes the same value at any two points which are symmetric with respect to ω_2. For more detailed discussions of $\wp(z|\omega_1,\omega_3)$, the reader is referred to the textbooks of Markushevich[18] and Ahlfors.[19]

A. Rectangular unit cell

We first assume that $\omega_1=\alpha$, $\omega_3=i\beta$ $(\alpha,\beta>0)$ and that the slit $\Omega=\{x_1+i\beta : \alpha-\alpha_0<x_1<\alpha+\alpha_0\}$ $(0<\alpha_0<\alpha)$ lies on the horizontal line $\mathrm{Im}[z]=\beta$. In this case, Y is an open rectangular with base 2α and height 2β (see Fig. 2). We briefly write $\wp(z)=\wp(z|\omega_1=\alpha,\omega_3=i\beta)$ in this section. From Markushevich[18] we know that $\wp(z)$ takes real values on the vertical lines $\mathrm{Re}[z]=\alpha$ and horizontal lines $\mathrm{Im}[z]=\beta$ and nonreal values otherwise on the parallelogram Y. Further, $[0,\alpha]\ni x\mapsto\wp(x+i\beta)$ $([0,\beta]\ni x\mapsto\wp(\alpha+ix))$ is strictly increasing (decreasing). Let $e_i=\wp(\omega_i)$ $(i=1,2,3)$. Clearly, $e_3<e_2<e_1$ and

$$\wp(\alpha-\alpha_0+i\beta)=\wp(\alpha+\alpha_0+i\beta)=: e_{23}\in(e_3,e_2) \tag{23}$$

is a real number between e_3 and e_2. Let $\Omega_{\mathrm{per}}=\{z+\omega : z\in\Omega,\omega\in\mathcal{L}\}$ be the periodic extension of Ω. Following Ref. 17, we define

$$\Psi(z)=\int_{\gamma(0,z)}\phi(z_1)dz_1 =: U(x_1,x_2)+iV(x_1,x_2),\qquad \phi(z)=\sqrt{\frac{\wp(z)-e_2}{\wp(z)-e_{23}}}, \tag{24}$$

where $\gamma(0,z)$ denotes a rectifiable integration path contained in $\mathbb{C}\setminus\bar{\Omega}_{\mathrm{per}}$, $U(V):IR^2\setminus\bar{\Omega}_{\mathrm{per}}\to IR$ is the real (imaginary) part of Ψ, and the square root takes values only from the branch with $\sqrt{1}=1$ (the branch cut is along the negative real axis). Grabovsky and Kohn[17] showed that $\Psi(z)$ is single-valued, analytic on $\mathbb{C}\setminus\bar{\Omega}_{\mathrm{per}}$, and hence satisfies the Cauchy–Riemann equation

$$\frac{\partial U}{\partial x_1}=\frac{\partial V}{\partial x_2},\quad \frac{\partial U}{\partial x_2}=-\frac{\partial V}{\partial x_1}\quad\text{on}\quad \mathbb{C}\setminus\bar{\Omega}_{\mathrm{per}}. \tag{25}$$

Let

$$t_1 = \Psi(\alpha) = \int_{\gamma_1} \phi(z)dz \text{ and } it_3 = \Psi(i\beta) = \int_{\gamma_2} \phi(z)dz, \tag{26}$$

where $\gamma_1 = \{x_1 + ix_2 : 0 \le x_1 \le \alpha, x_2 = 0\}$ and $\gamma_2 = \{x_1 + ix_2 : 0 \le x_2 \le \beta, x_1 = 0\}$. Since $IR \ni \wp(z) \ge e_1$ on γ_1, $IR \ni \wp(z) \le e_3$ on γ_2, and $\mathrm{Re}[\phi(z)] = 0$ $\forall z \in \Omega$, we see that $t_1, t_3 > 0$,

$$\frac{\partial U(x_1,x_2)}{\partial x_1} = \frac{\partial V(x_1,x_2)}{\partial x_2} = 0 \quad \forall (x_1,x_2) \in \partial\Omega. \tag{27}$$

In particular, we notice that U is continuous on IR^2, but V is discontinuous across the slit Ω. Since $d/dz[\Psi(z+2\alpha) - \Psi(z)] = 0$ and $d/dz[\Psi(z+2i\beta) - \Psi(z)] = 0$, by Eq. (26) we have

$$\left.\begin{array}{l}\Psi(z+2\alpha) = \Psi(z) + 2t_1 \\ \Psi(z+2i\beta) = \Psi(z) + 2it_3\end{array}\right\} \quad \forall z \in \mathbb{C} \setminus \bar{\Omega}_{\text{per}}. \tag{28}$$

From Eq. (28) and the first of Eq. (24), we obtain

$$U(0,x_2) = U(2\alpha,x_2) - 2t_1, \quad V(0,x_2) = V(2\alpha,x_2), \quad \forall x_2 \in [0,2\beta],$$

$$U(x_1,0) = U(x_1,2\beta), \quad V(x_1,0) = V(x_1,2\beta) - 2t_3, \quad \forall x_1 \in [0,2\alpha]. \tag{29}$$

We claim that

$$u_{\mathbf{f}}(x_1,x_2) = \frac{\alpha f_1}{t_1} U(x_1,x_2) - f_1 x_1 \quad \forall (x_1,x_2) \in Y \setminus \bar{\Omega} \tag{30}$$

is a solution of Eq. (17). To show this, we notice that $u_{\mathbf{f}}$ defined by Eq. (30) satisfies the first and second of Eq. (17) [see Eqs. (18) and (27)]. The last of Eq. (17), i.e.,

$$u_{\mathbf{f}}(0,x_2) = \frac{f_1\alpha}{t_1} U(0,x_2) = \frac{f_1\alpha}{t_1} U(2\alpha,x_2) - 2f_1\alpha = u_{\mathbf{f}}(2\alpha,x_2) \quad \forall x_2 \in [0,2\beta],$$

$$u_{\mathbf{f}}(x_1,0) = \frac{f_1\alpha}{t_1} U(x_1,0) = \frac{f_1\alpha}{t_1} U(x_1,2\beta) = u_{\mathbf{f}}(x_1,2\beta) \quad \forall x_1 \in [0,2\alpha], \tag{31}$$

follows from Eq. (29).

We now calculate the effective conductivity tensor $\mathbf{A}^e$. Note that Eq. (6) is not applicable for $k_1 = \infty$ and $\theta = 0$, and we shall use Eq. (5). From Eqs. (25), (29), and (30) we find

$$\begin{aligned}\mathbf{f} \cdot \mathbf{A}^e \mathbf{f} &= \frac{1}{4\alpha\beta} \int_{\partial Y} (\mathbf{f} \cdot \mathbf{x}) \mathbf{n} \cdot \mathbf{A}(\mathbf{x})(\nabla u_{\mathbf{f}} + \mathbf{f}) \\ &= \frac{k_0}{4\alpha\beta} \left[\int_0^{2\alpha} 2\beta f_2 \left(\frac{\partial u_{\mathbf{f}}}{\partial x_2} + f_2 \right) dx_1 + \int_0^{2\beta} 2\alpha f_1 \left(\frac{\partial u_{\mathbf{f}}}{\partial x_1} + f_1 \right) dx_2 \right] \\ &= k_0 f_2^2 + \frac{k_0}{4\alpha\beta} \frac{\alpha f_1}{t_1} \left[\int_0^{2\alpha} 2\beta f_2 \frac{\partial U}{\partial x_2} dx_1 + \int_0^{2\beta} 2\alpha f_1 \frac{\partial U}{\partial x_1} dx_2 \right] \\ &= k_0 f_2^2 + \frac{k_0}{4\alpha\beta} \frac{\alpha f_1}{t_1} [-2\beta f_2 V(x_1,x_2)|_{x_1=0}^{x_1=2\alpha} + 2\alpha f_1 V(x_1,x_2)|_{x_2=0}^{x_2=2\beta}] = k_0 \left(f_2^2 + f_1^2 \frac{\alpha t_3}{\beta t_1} \right).\end{aligned}$$

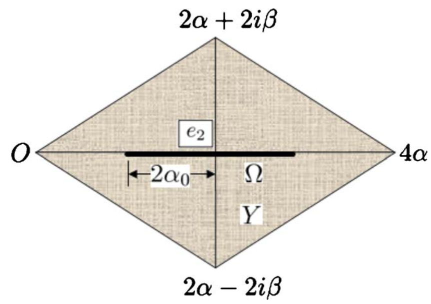

FIG. 3. (Color online) Rhombic unit cell.

That is,

$$\frac{1}{k_0} \mathbf{A}^e = \begin{bmatrix} \frac{\alpha t_3}{\beta t_1} & 0 \\ 0 & 1 \end{bmatrix}. \tag{32}$$

It is convenient to relate the effective conductivity directly with the geometric parameters, e.g., the length of the slit $2\alpha_0$. To this end, we note that (see Ref. 18)

$$\left[\frac{d\wp(z)}{dz}\right]^2 = 4[\wp(z) - e_1][\wp(z) - e_2][\wp(z) - e_3],$$

$$\alpha = \frac{1}{\sqrt{e_1 - e_3}} K\left(\frac{e_2 - e_3}{e_1 - e_3}\right), \quad \beta = \frac{1}{\sqrt{e_1 - e_3}} K\left(\frac{e_1 - e_2}{e_1 - e_3}\right), \tag{33}$$

where

$$K(m) = \int_0^1 \frac{dt}{(1-t^2)(1-mt^2)}$$

is the complete elliptic integral of the first kind. Changing the integration variable from z to $\wp = \wp(z)$, by Eq. (33) we write Eq. (26) as

$$t_1 = \int_{e_1}^{+\infty} \frac{1}{\sqrt{4(\wp - e_1)(\wp - e_{23})(\wp - e_3)}} d\wp = \frac{1}{\sqrt{e_1 - e_3}} K\left(\frac{e_{23} - e_3}{e_1 - e_3}\right),$$

$$t_3 = \int_{-\infty}^{e_3} \frac{1}{\sqrt{-4(\wp - e_1)(\wp - e_{23})(\wp - e_3)}} d\wp = \frac{1}{\sqrt{e_1 - e_3}} K\left(\frac{e_1 - e_{23}}{e_1 - e_3}\right). \tag{34}$$

Therefore,

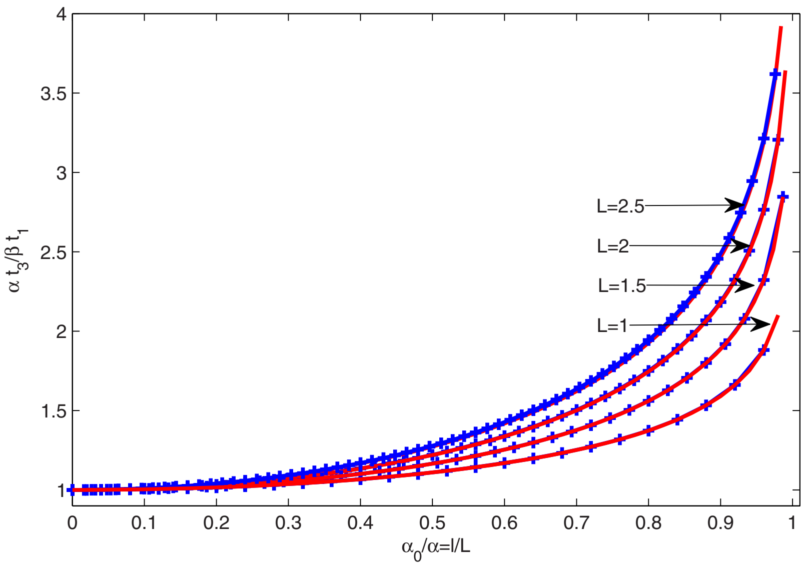

FIG. 4. (Color online) The effective conductivity in x_1-direction vs the length of the slit. From up to down, the unmarked curves are calculated for rectangular unit cells with $2\beta=d=2$ and $2\alpha=L=2.5,2,1.5,1$. The + markers are calculated for rhombic unit cells with $2\beta=d=2$ and $4\alpha=L=2.5,2,1.5,1$ (see also Figs. 8 and 9).

$$\frac{\alpha t_3}{\beta t_1}=\frac{K(m_0)K(1-m')}{K(1-m_0)K(m')}, \quad m_0=\frac{e_2-e_3}{e_1-e_3}, \quad m'=\frac{e_{23}-e_3}{e_1-e_3}. \tag{35}$$

We now discuss how the effective conductivity depends on the geometric parameters of the microstructures. First, let us fix the unit cell and calculate $\alpha t_3/\beta t_1$ as a function of α_0. Setting $\beta=d/2$ and $\alpha=L/2$, we have periodic slits as shown in Fig. 8. By Eqs. (34) and (35) we compute $\alpha t_3/\beta t_1$ versus $\alpha_0\in(0,1)$ shown by the unmarked curves in Fig. 4. From up to down, the curves are calculated for $\beta=1$ and $2\alpha=L=2.5,2,1.5,1$. Immediately, we see the effective conductivity along x_1-direction increases from one to infinity as the length of the slit increases from 0 to 2α. In Fig. 5 we set $\alpha=1$ and compute $\alpha t_3/\beta t_1$ versus $\beta\in(0,1)$. From up to down, the half length of the slit, α_0, is 0.9, 0.8, and 0.4. We see that the larger β is, the smaller effect the perfectly conducting slits have on the effective conductivity. In the limit of $\beta\to+\infty$, the effective conductivity of the composite shall be the same as the matrix if $\alpha_0\neq\alpha$. To measure the effect of the slits in this limit, we define a dimensionless quantity

$$\delta=\lim_{\beta\to+\infty}\frac{\beta}{\alpha}\left[\frac{\alpha t_3(\alpha,\beta,\alpha_0)}{\beta t_1(\alpha,\beta,\alpha_0)}-1\right].$$

Physically $k_0\delta\alpha^2 f_1^2$ can be interpreted as the energy of the stray field of an infinite vertical strip of width 2α in the presence of a periodic array of perfectly conducting slits and under the application a uniform far field $\mathbf{f}=(f_1,f_2)$. By dimensional analysis we infer $\delta=\delta(\alpha_0/\alpha)$. An analytic expression of it is desirable but not obvious. We turn to numerical method. Figure 6 shows the curve $\delta=\delta(\alpha_0/\alpha)$. Finally, we plot the local field in the unit cell for $\alpha=\beta=1$ and $\alpha_0=0.8$ in Fig. 7. We remark that the field is in fact singular around the two tips of the slit as if there are static and opposite signed charges concentrated at the two tips.

We now consider the case $k_1=0$. Similarly, from Eqs. (27) and (29) we verify that

$$u_{\mathbf{f}}(x_1,x_2)=\frac{f_2\beta}{t_3}V(x_1,x_2)-f_2x_2 \quad \forall\ (x_1,x_2)\in Y\setminus\bar{\Omega} \tag{36}$$

satisfies all of Eq. (19). Since $k_1=0$ and $\theta=0$, from the last line of Eq. (6) we have

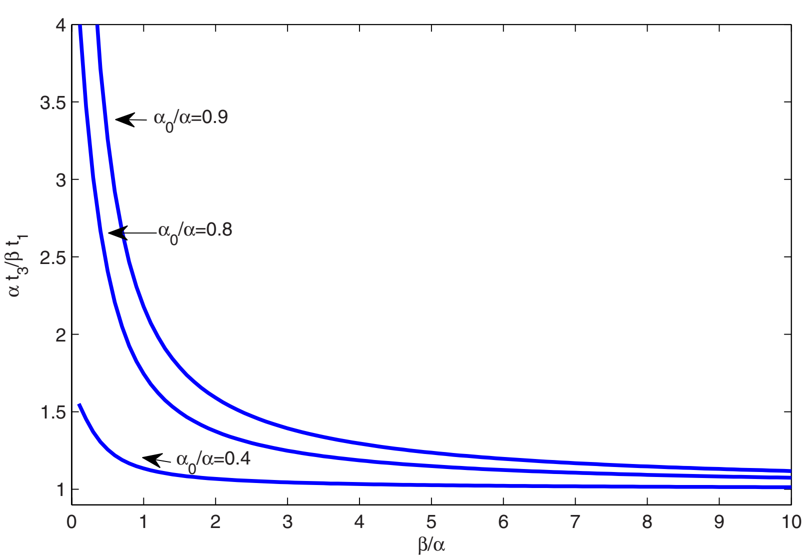

FIG. 5. (Color online) The effective conductivity in x_1-direction vs the aspect ratio of the rectangular unit cell. From up to down, the curves are calculated for $\alpha=1$ and $\alpha_0=0.9,0.8,0.4$.

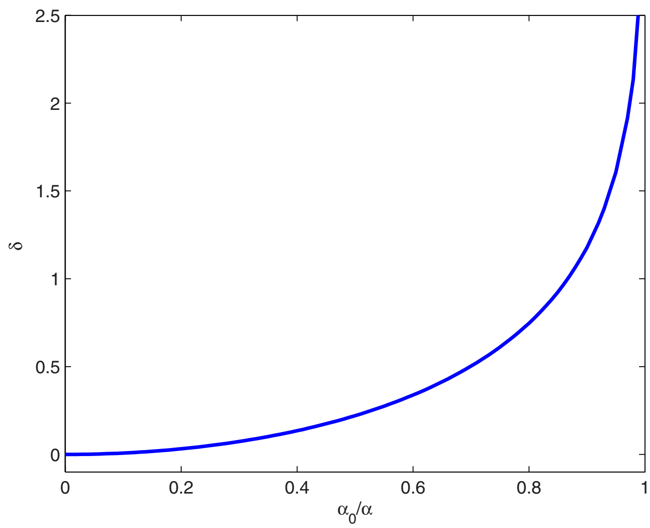

FIG. 6. (Color online) The dimensionless quantity δ vs α_0/α.

$$\mathbf{f}\cdot\mathbf{A}^e\mathbf{f}=k_0|\mathbf{f}|^2+k_0\mathbf{f}\cdot\int_{Y\setminus\Omega}\nabla u_{\mathbf{f}}. \tag{37}$$

To find the unknown integral on the right hand side of Eq. (37), we notice that from the Green's theorem or the divergence theorem,

$$\int_{\partial Y}\begin{bmatrix} iU \\ U\end{bmatrix}\cdot\mathbf{n}ds=\int_{Y\setminus\Omega}\left[\frac{\partial U}{\partial x_2}+i\frac{\partial U}{\partial x_1}\right]dx_1dx_2 + \int_{\partial\Omega}\begin{bmatrix} iU \\ U\end{bmatrix}\cdot\mathbf{n}ds, \tag{38}$$

where $(ds)^2=(dx_1)^2+(dx_2)^2$ and $\mathbf{n}$ is the outward normal on ∂Y or $\partial\Omega$. Since U is continuous and bounded on Y, the last term on the right hand side of Eq. (38) vanishes. From Eqs. (25), (29), and (38) we obtain

$$\int_{Y\setminus\Omega}\left[-\frac{\partial V}{\partial x_1}+i\frac{\partial V}{\partial x_2}\right]dx_1dx_2=\int_{\partial Y}\begin{bmatrix} iU \\ U\end{bmatrix}\cdot\mathbf{n}ds=4it_1\beta. \tag{39}$$

From Eqs. (36) and (37) we conclude that

$$\mathbf{f}\cdot\mathbf{A}^e\mathbf{f}=k_0\left[|\mathbf{f}|^2+f_2^2\left(\frac{\beta t_1}{\alpha t_3}-1\right)\right]\Rightarrow\frac{1}{k_0}\mathbf{A}^e=\begin{bmatrix}1 & 0\\ 0 & \dfrac{\beta t_1}{\alpha t_3}\end{bmatrix}. \tag{40}$$

We remark that Eq. (40) can also be obtained from Eq. (32) by the duality transformation.[4,5,15]

B. Rhombic unit cell

In this section we assume that $\omega_1=\alpha-i\beta$, $\omega_2=2\alpha$, and $\omega_3=\alpha+i\beta$ $(\alpha,\beta>0)$ and that the slit $\Omega=\{x_1:2\alpha-\alpha_0<x_1<2\alpha+\alpha_0\}$ $(0<\alpha_0<2\alpha)$ lies on the x_1-axis (see Fig. 3). In this case, Y is an open rhombus with side length of $2(\alpha^2+\beta^2)^{1/2}$ and area of $8\alpha\beta$. We again briefly write $\wp(z)=\wp(z|\omega_1=\alpha-i\beta,\omega_3=\alpha+i\beta)$. Accordingly, we use the same

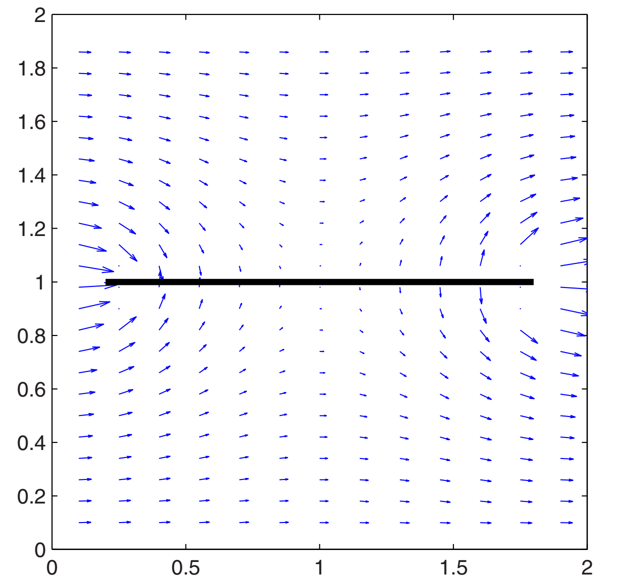

FIG. 7. (Color online) The electric field in the unit cell for $\alpha=\beta=1$ and $\alpha_0=0.8$.

notations in this section for the same type of quantities as in the last section. Within the context this shall not give rise to confusion.

From Markushevich[18] we know that $\wp(z)$ takes real values on the vertical lines $\mathrm{Re}[z]=2\alpha$ and horizontal lines $\mathrm{Im}[z]=0$ and nonreal values otherwise on the open parallelogram Y. Let $e_i=\wp(\omega_i)$. We further know that $e_1=\bar{e}_3$ is not a real number and $(0,2\alpha]\ni x\mapsto\wp(x)$ strictly decreases from $+\infty$ to e_2. Let

$$e_{23}=\wp(2\alpha-\alpha_0)=\wp(2\alpha+\alpha_0)\in(e_2,+\infty)$$

and define, as in Eq. (24),

$$\Psi(z)=\int_{\gamma(0,z)}\phi(z_1)dz_1=:U(x_1,x_2)+iV(x_1,x_2),\quad \phi(z)=\sqrt{\frac{\wp(z)-e_2}{\wp(z)-e_{23}}}. \tag{41}$$

We can similarly verify that $\Psi(z)$ is single-valued, analytic on $\mathbb{C}\setminus\bar{\Omega}_{\mathrm{per}}$, and hence satisfies the Cauchy–Riemann Eq. (25) on $\mathbb{C}\setminus\bar{\Omega}_{\mathrm{per}}$. Let

$$t_1-it_3=\tfrac{1}{2}\Psi(2\alpha-2i\beta)=\tfrac{1}{2}\int_{\gamma_1}\phi(z)dz, \tag{42}$$

where γ_1 is the straight path from 0 to $2\omega_1=2\alpha-2i\beta$. Since $\overline{\wp(z)}=\wp(\bar{z})$ and $\overline{\sqrt{z}}=\sqrt{\bar{z}}$, we have

$$t_1+it_3=\tfrac{1}{2}\Psi(2\alpha+2i\beta)=\tfrac{1}{2}\int_{\gamma_2}\phi(z)dz, \tag{43}$$

where γ_2 is the straight path from 0 to $2\omega_3=2\alpha+2i\beta$. Let $\gamma_3=\{x:0\le x\le 2\alpha-\alpha_0\}$. Since $\mathrm{Im}[\phi(z)]=0$ on γ_3 and $\mathrm{Re}[\phi(z)]=0$ on Ω, we have

$$\frac{\partial U(x_1,x_2)}{\partial x_1}=\frac{\partial V(x_1,x_2)}{\partial x_2}=0\qquad\forall\,(x_1,x_2)\in\partial\Omega. \tag{44}$$

Analogous to Eqs. (28)–(40), we again find that

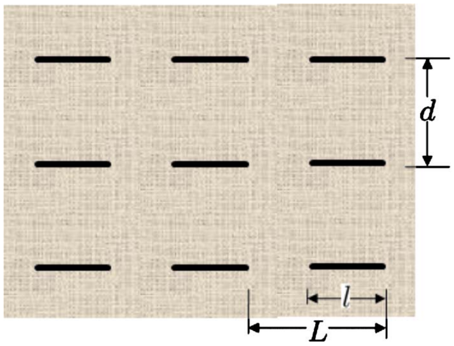

FIG. 8. (Color online) Periodic slits arranged in a rectangular lattice.

$$u_{\mathbf{f}}(x_1,x_2) = \frac{\alpha f_1}{t_1}U(x_1,x_2) - f_1 x_1 \quad \forall\ (x_1,x_2) \in Y \setminus \bar{\Omega}$$

is a solution of Eq. (17), and therefore,

$$\frac{1}{k_0}\mathbf{A}^e = \begin{bmatrix} \dfrac{\alpha t_3}{\beta t_1} & 0 \\ 0 & 1 \end{bmatrix}. \quad (45)$$

The reader is invited to carry out the detailed calculations. More, from Ref. 18 we find

$$\frac{\alpha}{\beta} = \frac{\displaystyle\int_0^\infty \frac{dt}{\sqrt{t^4 + 2t^2 \cos \varphi_0 + 1}}}{\displaystyle\int_0^\infty \frac{dt}{\sqrt{t^4 - 2t^2 \cos \varphi_0 + 1}}}, \quad \exp(2i\varphi_0) = \frac{e_2 - e_1}{e_2 - e_3},$$

$$\frac{t_1}{t_3} = \frac{\displaystyle\int_0^\infty \frac{dt}{\sqrt{t^4 + 2t^2 \cos \varphi' + 1}}}{\displaystyle\int_0^\infty \frac{dt}{\sqrt{t^4 - 2t^2 \cos \varphi' + 1}}}, \quad \exp(2i\varphi') = \frac{e_{23} - e_1}{e_{23} - e_3}, \quad (46)$$

where $0 < \varphi_0, \varphi' < \pi$.

To investigate the effects of different lattices or unit cells, we compare the following two configurations (see Figs. 8 and 9). It is not hard to see that the periodic slits in Fig. 8 correspond to a rectangular unit cell in Fig. 2 with $\alpha = L/2$, $\beta = d/2$, and $\alpha_0 = l/2$, whereas the periodic slits in Fig. 9 correspond to a rhombic unit cell in Fig. 3 with $\alpha = L/4$, $\beta = d/2$, and $\alpha_0 = l/4$. Meanwhile, if we shift to the left by $L/2$ every other layer of the slits in Fig. 8, we obtain the configuration in Fig. 9. Using Eqs. (35) and (46), in Fig. 4 we plot the effective conductivities along x_1-direction of these two configurations against l/L by unmarked curve and "+" markers, respectively. From up to down, the geometric parameters in Figs. 8 and 9 are chosen as $d=2$, $l=1$, and $L=2.5, 2, 1.5, 1$. We observe that there is no discernible difference between the unmarked curve and + markers in Fig. 4, which means the effective conductivities of the two configurations in Figs. 8 and 9 are the same, at least to the extent of our numerical resolution. The reader may speculate that this arises from symmetry; the author remarks that elementary arguments by symmetry cannot prove this unexpected result.

For the case $k_1 = 0$, by similar arguments we verify that

$$u_{\mathbf{f}}(x_1,x_2) = \frac{f_2 \beta}{t_3}V(x_1,x_2) - f_2 x_2 \quad \forall\ (x_1,x_2) \in Y \setminus \bar{\Omega} \quad (47)$$

satisfies all of Eq. (19). Parallel to Eqs. (37)–(40) or simply by the duality transformation, we can show the effective con-

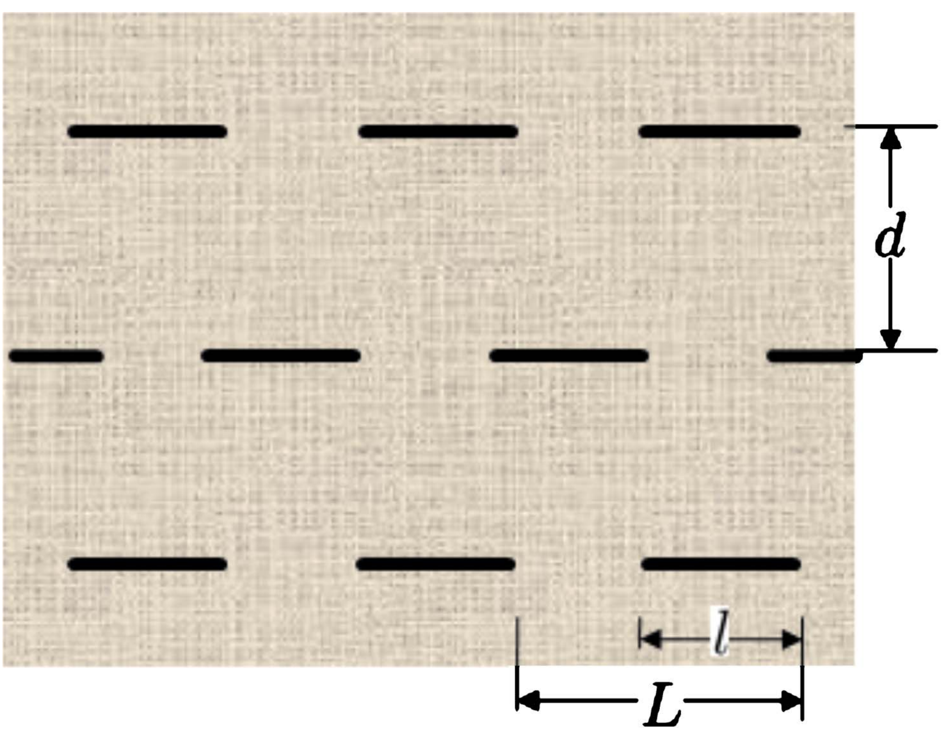

FIG. 9. (Color online) Periodic slits arranged in a rhombic lattice.

ductivity is given by Eq. (40) with α, β, t_1, and t_3 interpreted as in Eq. (45).

V. SUMMARY AND DISCUSSION

We derive a closed-form formula for the effective conductivity of composites with periodic E-inclusion microstructure. When the periodic E-inclusion degenerates to a periodic array of slits, we give explicit solutions to local fields and the effective conductivity of the composite with singular inhomogeneities. Through a linear transformation, these results can be extended to two-phase composites of any anisotropic materials.

The results of this paper can be used in the following ways. In the first place the closed-form formula (13) with the volume fraction θ and the shape matrix $\mathbf{Q}$ as parameters can be used to give a quick estimate of the effective properties of a composite. In reality, of course, it is questionable to what extent the microstructure of a composite can be approximated by a periodic E-inclusion. However our prediction [see Eq. (13)] is at least physical and realizable, and the qualitative feature of how the effective properties depend on the volume fraction and shape of the inhomogeneities should remain regardless of the exact shapes of the inhomogeneities. Second, the analytic results provide a benchmark for testing various empirical models and numerical codes. Last but not least important, the results in Sec. IV, in particular the comparison between rectangular and rhombic unit cells (see Fig. 4), suggest that the effective properties of composites with a singular phase are predominantly determined by the distance between nearby inhomogeneities. This has been observed by various authors and is in fact the basis of the network model.[6–9] What is noteworthy here is that this remains to be true even for an extreme shape such as a slit, for which the field is not localized between slits (see Fig. 7).

[1] D. J. Bergman, Phys. Rep., Phys. Lett. **43**, 377 (1978).
[2] R. Hill, J. Mech. Phys. Solids **13**, 213 (1965).
[3] Z. Hashin and S. Shtrikman, J. Appl. Phys. **33**, 3125 (1962).
[4] J. B. Keller, J. Appl. Phys. **34**, 991 (1963).
[5] A. Dykne, Sov. Phys. JETP **32**, 63 (1971).
[6] V. Ambegaokar, B. I. Halperin, and J. S. Langer, Phys. Rev. B **4**, 2612 (1971).
[7] J. P. Clerc, G. Giraud, J. M. Laugier, and J. M. Luck, Adv. Phys. **39**, 191–309 (1990).
[8] S. M. Kozlov, Russ. Math. Surv. **44**, 91 (1989).
[9] L. Berlyand and A. Kolpakov, Arch. Ration. Mech. Anal. **159**, 179 (2001).
[10] W. R. Delameter, G. Herrmann, and D. M. Barnett, ASME Trans. J. Appl. Mech. **42**, 74 (1975).
[11] J. Wang, J. Fang, and B. L. Karihaloo, Int. J. Solids Struct. **37**, 4261 (2000).
[12] S. B. Vigdergauz, Inzh. Zh., Mekh. Tverd. Tela **21**, 165–169 (1986).
[13] L. P. Liu, R. D. James, and P. H. Leo, Arch. Ration. Mech. Anal. (unpublished).
[14] A. Friedman, *Variational Principles and Free Boundary Problems* (Wiley, New York, 1982).
[15] G. W. Milton, *The Theory of Composites* (Cambridge University Press, Cambridge, 2002).
[16] L. P. Liu, R. D. James, and P. H. Leo, Metall. Mater. Trans. A **38**, 781 (2007).
[17] Y. Grabovsky and R. V. Kohn, J. Mech. Phys. Solids **43**, 949 (1995).
[18] A. I. Markushevich, *Theory of Function of Complex Variable* (Chelsea, New York, 1977), Vol. 1–3.
[19] L. V. Ahlfors, *Complex Analysis* (McGraw-Hill, New York, 1979).